Research Square

Preprints are preliminary reports that have not undergone peer review.
They should not be considered conclusive, used to inform clinical practice,
or referenced by the media as validated information.

RadMaps: A Geospatial Framework for Simultaneously Modelling Capacity and Geographic Constraints on Radiotherapy Access

Laurence Wroe

laurencewroe@gmail.com

Exceleray Sàrl

Archie Brown

University of Oxford

Sophia Martin

University of Oxford

Alika Ho

University of Oxford

Steinar Stapnes

University of Oslo

Research Article

Keywords:

Posted Date: June 1st, 2026

DOI: https://doi.org/10.21203/rs.3.rs-9772089/v1

License: This work is licensed under a Creative Commons Attribution 4.0 International License.
Read Full License

Additional Declarations: No competing interests reported.

RadMaps: A Geospatial Framework for Simultaneously Modelling Capacity and Geographic Constraints on Radiotherapy Access

Laurence Wroe[a], Archie Brown[b], Sophia Martin[b], Alika Ho[b], Steinar Stapnes[a,c]

[a]*Exceleray Sàrl, Versoix, Geneva, 1290, Switzerland*
[b]*Department of Physics, University of Oxford, Keble Road, Oxford, OX1 3RH, United Kingdom*
[c]*Department of Physics, University of Oslo, Sem Sælands vei 24, Oslo, 0371, Norway*

Abstract

Background: Access to radiotherapy is constrained by two compounding factors: insufficient machine capacity to meet patient demand and geographic distance from treatment facilities. Existing analyses address these factors separately, constraining the insights available to planners and policymakers. This paper presents RadMaps, an open-source geospatial framework that simultaneously models capacity and geographic constraints on radiotherapy access at any spatial scale.

Methods: RadMaps operates on Uber's H3 hexagonal grid and integrates population density data with national cancer incidence estimates and radiotherapy facility inventories. Radiotherapy demand is estimated using cancer-site-specific radiotherapy utilisation rates, and geographic access is modelled via configurable decay functions (uniform, step, or Weibull) using either distance, driving time, or public transport time, with travel times obtained via the TravelTime API. A greedy nearest-first allocation algorithm assigns demand to facilities subject to both capacity and geographic constraints, producing a localised access metric for every H3 hexagon.

Results: Applied globally at H3 Resolution-3 with a 200 km step-function threshold, RadMaps computes a capacity-only access of 70 %, a geography-only access of 91 %, and a combined radiotherapy access of 60 %, illustrating

Email address: laurencewroe@gmail.com (Laurence Wroe)

the compounding effect of capacity and geographic constraints to significantly reduce effective access. High-resolution analyses of six countries (Australia, India, Nigeria, Oman, the United Kingdom, and the United States) demonstrate the tool's ability to localise access deficits at sub-national scale and reveal distinct access profiles: capacity-limited (United Kingdom), geographically-limited (Oman), and doubly-constrained (India and Nigeria)
Conclusions: RadMaps provides a flexible, open-access framework for visualising and identifying radiotherapy access gaps at regional to global scales, with applications in infrastructure planning and policy prioritisation. RadMaps' modular framework is also readily extensible to other spatial access modelling applications.

---

1. Background

1.1. Introduction

Cancer is a leading cause of mortality worldwide, with an estimated 20 million new cases and 9.7 million deaths in 2022, projected to rise to approximately 35 million annual cases by 2050 (Bray et al., 2024). One of the principal treatment modalities for cancer is radiotherapy, which is required by approximately half of all patients for curative, adjuvant, or palliative purposes (Delaney et al., 2005; Barton et al., 2014). There is, however, a well-recognised global shortfall of access to radiotherapy, driven by two compounding constraints.

The first is a *capacity constraint*. The majority of radiotherapy is delivered via external beam radiotherapy (EBRT), in which a megavoltage machine (MVM) — predominantly a linear accelerator (linac) — delivers a targeted beam of ionising radiation to damage cancer cells (Healy et al., 2017). Operating these machines is resource-intensive: linacs are expensive, require stable local infrastructure, dedicated shielding, and ongoing maintenance, and their clinical operation requires a multidisciplinary team of oncologists, medical physicists, dosimetrists, nurses, and engineers (Dunscombe et al., 2014). Using a commonly accepted benchmark of treating 450 patients per machine per year (Zubizarreta et al., 2015), the global fleet of approximately 17,000 machines falls well short of demand. This represents an immediate shortfall of roughly 7,000 based on current case volumes, with long-term projections suggesting that an additional 30,470 linacs will be required by 2045 to keep pace with growing global demand (Moraes et al., 2025).

The second is a *geographic constraint*. Treatment is typically delivered in daily fractions (individual treatment sessions) over several weeks. This can place a strain on populations living far from a facility, who may therefore receive suboptimal treatment or none at all (Silverwood et al., 2024). A recent geospatial analysis found that 76 % of the global population lives within 2 h of travel time to a radiotherapy facility, with this figure dropping to 17 % in low-income countries (Wawrzuta et al., 2025).

In practice, these two constraints interact. Capacity-based analyses, which compare national demand with total machine counts, provide a valuable picture of the theoretical shortfall but do not capture the reduced access faced by populations far from any facility. Geographic-based analyses, such as that of Wawrzuta et al. (Wawrzuta et al., 2025), illustrate the proximity to and distribution of facilities but do not account for the finite capacity of individual machines. Modelling both constraints simultaneously offers a more complete picture of radiotherapy access. To our knowledge, no existing tool simultaneously models both constraints on a continuous multi-scale, multi-national spatial framework.

This paper presents RadMaps, an open-source geospatial tool that simultaneously models capacity and geographic constraints on radiotherapy access at any spatial scale, from sub-national to global. The tool operates on a hexagonal spatial grid and combines high-resolution population density data with national site-specific cancer incidence estimates, radiotherapy facility inventories and locations, and configurable geographic access decay functions. We describe the methodology, evaluate it through demonstration across a range of geographic and socioeconomic contexts, and discuss limitations and directions for future work.

2. Methods

2.1. Spatial Framework

RadMaps operates on H3, a hierarchical geospatial indexing system developed by Uber that partitions the globe into hexagonal cells at 16 discrete resolutions (Uber, 2025). H3 offers several advantages over administrative boundaries or rectangular grids for spatial accessibility analysis including: each hexagonal cell has an approximately equal distance from its centroid to all six neighbouring centroids, reducing directional bias; cell areas remain near-uniform across latitudes, with the ratio of largest to smallest cell area

below 2:1 at all resolutions; and the hierarchical structure allows efficient aggregation across resolutions. RadMaps supports resolutions from Resolution-3 (average cell area of 12 400 km^2) down to Resolution-7 (5.16 km^2).

2.2. Data Sources

RadMaps uses three primary datasets.

Population. Population density data are taken from the Kontur Global Population Density dataset (Kontur, Inc., 2023), which provides population estimates at H3 Resolution-8, integrating data from multiple sources covering the period March 2020 to November 2023. Population data are aggregated into parent hexagons at the chosen resolution in line with the H3 hierarchy.

Cancer Incidence. Cancer incidence estimates for 36 different cancer types across 185 countries are taken from GLOBOCAN 2022 (Bray et al., 2024).

Radiotherapy Facilities. Facility-level data were obtained from the IAEA DIRAC database, which includes centre names, country, and inventories (International Atomic Energy Agency, 2025). The database utilised in RadMaps contains 8,592 radiotherapy facilities, 8,471 of which operate at least 1 MVM, for a total of 17,097 MVMs. For the purposes of modelling, all MVMs are treated as equivalent linacs with a default capacity of 450 patients per machine per year. Geographic coordinates were added to each facility by geocoding addresses against OpenStreetMap and Google Maps.

Travel Time. RadMaps supports geographic access modelling based on distance, driving time, or public transport time. While distance is computed directly within the H3 framework, driving and public transport times are integrated via TravelTime's H3 API (TravelTime, 2026), using typical traffic conditions departing at 08:00 on a Wednesday.

2.3. Radiotherapy Demand Estimation

The radiotherapy demand is calculated as

$$D = \sum_i \lambda_i I_i, \tag{1}$$

where I_i is the incidence for cancer site i and λ_i is the radiotherapy utilisation (RTU) rate for the cancer site.

The RTU is specified using one of three approaches:

- **Site-specific optimal RTU:** Cancer incidence per site is multiplied by the corresponding optimal radiotherapy utilisation rates as defined by Delaney et al. (Delaney et al., 2005).
- **Site-specific custom RTU:** Cancer incidence per site is multiplied by user-defined utilisation rates, allowing the model to reflect local clinical practise.
- **Proportional RTU:** Total cancer incidence is multiplied by a single user-defined factor, enabling rapid scenario testing where site-specific RTU is not applicable.

The resulting demand is then apportioned to individual hexagons to establish a local demand per hexagon D_h in proportion to their share of the total population.

2.4. Radiotherapy Access Modelling

RadMaps calculates three metrics for capturing access to radiotherapy: a capacity-only metric A_{C}, a geography-only metric A_{G}, and the RadMaps combined metric A_{RM} that accounts for both constraints simultaneously. Each is described in the following subsections.

2.4.1. Capacity-Only Access Metric

Radiotherapy machines are limited in the number of patients they can treat by operating hours, fractionation schedules, and uptime. RadMaps accounts for this by introducing a maximum throughput for each machine, which can be set in two ways:

- **Global:** A user-defined capacity constant C_{linac} is applied to all machines. The total capacity for a given facility is thus $C_{\mathrm{fac}} = N_{\mathrm{linac}} C_{\mathrm{linac}}$, where N_{linac} is the number of linacs at that site.
- **Custom:** Users can input specific capacities for individual centres, allowing the model to reflect local operational differences.

The default value is $C_{\mathrm{linac}} = 450$ patients per machine per year, consistent with established international benchmarks (Zubizarreta et al., 2015).

RadMaps then calculates capacity-only access and deficit as:

$$A_{\mathrm{C}} = \sum_{f} C_{\mathrm{fac},f}, \qquad \Delta_{\mathrm{C}} = D - A_{\mathrm{C}}, \tag{2}$$

where the sum is over all facilities f. A_{C} is capped at D, such that access cannot exceed demand.

2.4.2. Geography-Only Access Metric

The relationship between geographic access to radiotherapy and patient uptake and health outcomes is complex (Silverwood et al., 2024). While many studies demonstrate that increased travel distance or time is associated with reduced treatment uptake and poorer survival (Turner et al., 2023; Baade et al., 2011; Goyal et al., 2014), other research suggests a more nuanced picture where greater travel distances can even correlate with superior clinical outcomes (Turner et al., 2026). As there is no universal empirical consensus on a single access-decay curve, RadMaps allows users to define the geographic access variable x based on one of three metrics:

- **Distance:** The distance between the centroid of a given hexagon and a radiotherapy facility, computed directly within the H3 framework.
- **Driving time:** The mean duration of travel between a given hexagon and a radiotherapy facility by private car, integrated via the TravelTime API.
- **Public transport time:** The mean duration of travel using available public transit networks between a given hexagon and a radiotherapy facility, also integrated via the TravelTime API.

Given that the impact of travel burden varies significantly by context, RadMaps provides three configurable decay models:

- **Uniform:** $P(x) = 1$ for all hexagons, representing a scenario with no geographic barriers to radiotherapy access.
- **Step Function:** $P(x) = 1$ if $x \leq x_{\max}$, else $P(x) = 0$, where $x_{\max}$ is a hard catchment limit beyond which patients do not access radiotherapy.
- **Weibull:** $P(x) = \exp\left(-(x/\lambda)^k\right)$, where λ defines the scale of the decay and k the shape, allowing for smoother catchment modelling with softer limits.

In regions where a population in a given hexagon h is served by multiple facilities i, RadMaps calculates a cumulative geographic access probability

as:

$$P_h = 1 - \prod_i \big(1 - P(x_i)\big). \tag{3}$$

RadMaps calculates geography-only access and deficit as:

$$\mathrm{A_G} = \sum_h P_h \times \mathrm{D}_h, \qquad \Delta_\mathrm{G} = D - \mathrm{A_G}, \tag{4}$$

where D_h is the demand in hexagon h.

2.4.3. RadMaps Access Metric

The modelling pipeline RadMaps used to turn data sources and user inputs into radiotherapy access maps and metrics is summarised in Figure 1.

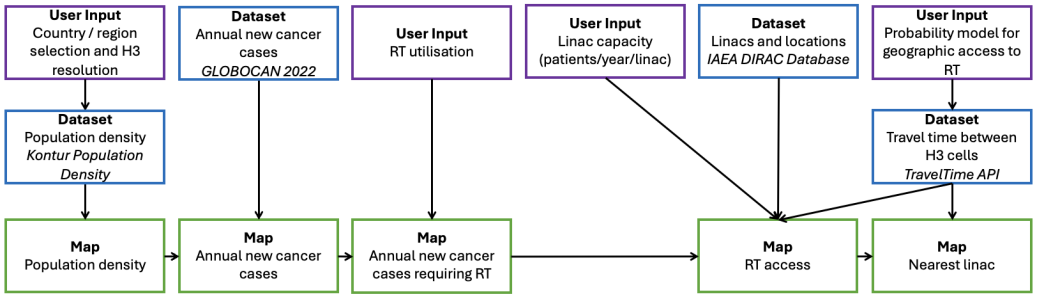


Figure 1: Modelling pipeline used by RadMaps to calculate radiotherapy access maps and metrics.

The algorithm processes radiotherapy access through the following steps:

1. **Sorting:** For each facility i, H3 hexagons are sorted by proximity (whether distance or travel time).
2. **Calculating Accessible Demand:** Starting with the nearest hexagon(s), the accessible demand is determined by multiplying the current radiotherapy demand D_h by the geographic access probability for that facility $P(x_i)$.
3. **Updating Capacity and Demand:** The accessible demand is subtracted from the facility's remaining capacity. Simultaneously, D_h is updated to reflect the demand that has accessed treatment. If a facility reaches its capacity limit, only the portion of demand that can be satisfied by the remaining capacity is subtracted.

4. **Termination:** This loop continues for each facility until either the facility's capacity is exhausted or the geographic access probabilities reach zero.

The greedy nearest-first allocation algorithm integrates local radiotherapy demand with both capacity and geographic constraints to produce localised access and deficit metrics A_h and Δ_h for every hexagon h. The RadMaps access and deficit are then calculated as:

$$\mathrm{A_{RM}} = \sum_h \mathrm{A}_h, \qquad \Delta_{\mathrm{RM}} = D - \mathrm{A_{RM}}. \tag{5}$$

While the approach relies on several assumptions discussed in section 4, this approach is computationally efficient, flexible, and can be applied consistently across any country or region.

2.5. Adding Facilities

To enable infrastructure scenario modelling, RadMaps allows user to add radiotherapy facilities and linacs. This can be done in one of two ways:

- **User-defined:** The user add radiotherapy centres in specific locations.
- **Automatic:** RadMaps places facilities in hexagons with the greatest unmet demand, with an option to lock onto existing facilities within a set distance or travel time.

In both cases, the algorithm is rerun following each addition, allowing users to evaluate the incremental impact of new facilities on access and deficit metrics.

2.6. Implementation

RadMaps is implemented in PYTHON as an open-source, open-access tool designed for use by any stakeholder involved or interested in radiotherapy access and planning. It is presented as an interactive dashboard using PYDECK with CARTO basemaps (CartoDB, 2018), with H3 hexagonal grids superimposed to visualise calculated demand and access metrics. The framework is modular and extensible, allowing users to adapt the underlying datasets and inputs for a more representative model. The entire codebase is hosted on GitHub at `https://github.com/LaurenceWroe/Geospatial-modelling-radiotherapy-access`, and the tool is currently accessible via a Streamlit web application at `https://rtaccess.streamlit.app/`.

3. Results

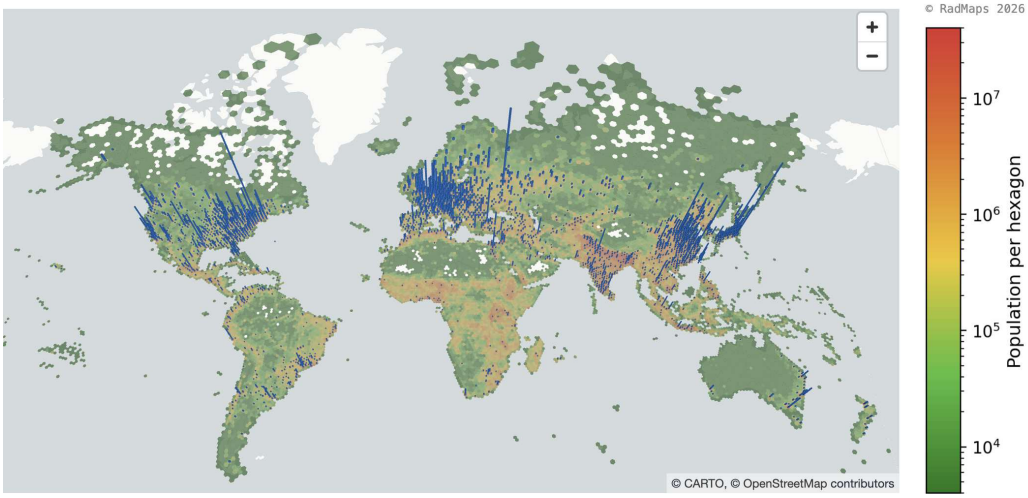
This section evaluates radiotherapy access using RadMaps, first at a global scale and then through high-resolution analyses of six countries (Australia, India, Nigeria, Oman, the United Kingdom, and the United States) representing a spectrum of geographic and socioeconomic contexts. All simulations assume optimal RTU rates and a default machine capacity of $C_{\text{linac}} = 450$ patients per linac per year.

3.1. Global Analysis

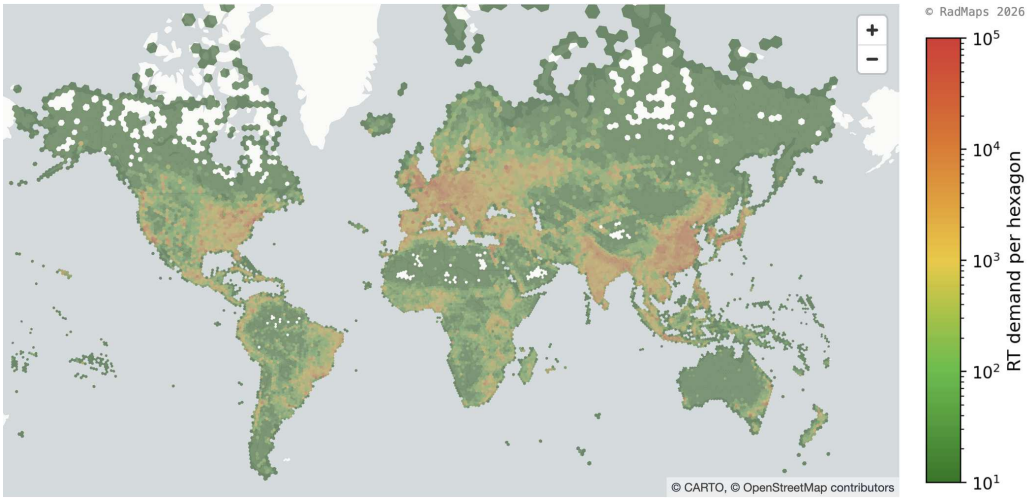
Figure 2 illustrates the global distribution of population density and radiotherapy demand at H3 Resolution-3 (cell areas ranging from 7730 km^2 to 15 000 km^2 with an average edge length of 69 km). Specifically, Figure 2a visualises the distribution of 8,471 radiotherapy facilities (housing 17,097 total linacs) superimposed on the global population of 8.02 billion. This mapping clearly highlights the denser concentration of radiotherapy facilities across North America, Europe, China, and Japan, in contrast to the sparsity across South America, Africa, and Southeast Asia. Figure 2b depicts the corresponding radiotherapy demand D_h, totalling 11.1 million. Here, demand is modelled independently for each country using national incidence rates; this captures distinct national demand profiles rather than assuming a uniform global distribution of cancer incidence, thereby reflecting the lower cancer incidence of regions such as Africa.

Figure 3 visualises the RadMaps radiotherapy deficit Δ_h and the access ratio A_h/D_h, assuming a 200 km step-function travel threshold. Comparing the demand in Figure 2b to the deficit in Figure 3a, we see that North America, Western Europe, and Australia are well-served with sufficient capacity and distribution of radiotherapy infrastructure to meet their national demand. In contrast, China, India, Southeast Asia, South America, the United Kingdom, and Sub-Saharan Africa contain large regions of deficit.

The local Δ_h metric primarily flags metropolitan areas where existing capacity is overwhelmed by demand. Consequently, vast, sparsely populated regions - such as the Sahara in Africa, the Outback in Australia, and the Amazon in South America - appear well-served simply because a low population density yields a low radiotherapy demand and consequently deficit. To better visualise the severe geographic isolation experiences by rural populations, Figure 3b shows the access ratio A_h/D_h per hexagon, and highlights



(a) Population density per hexagon and facility distribution.

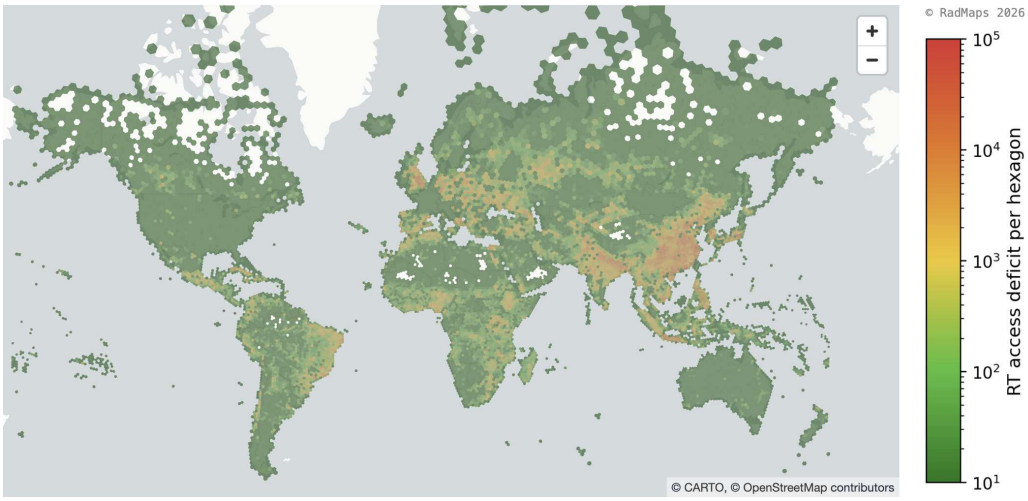


(b) Radiotherapy demand per hexagon, D_h.

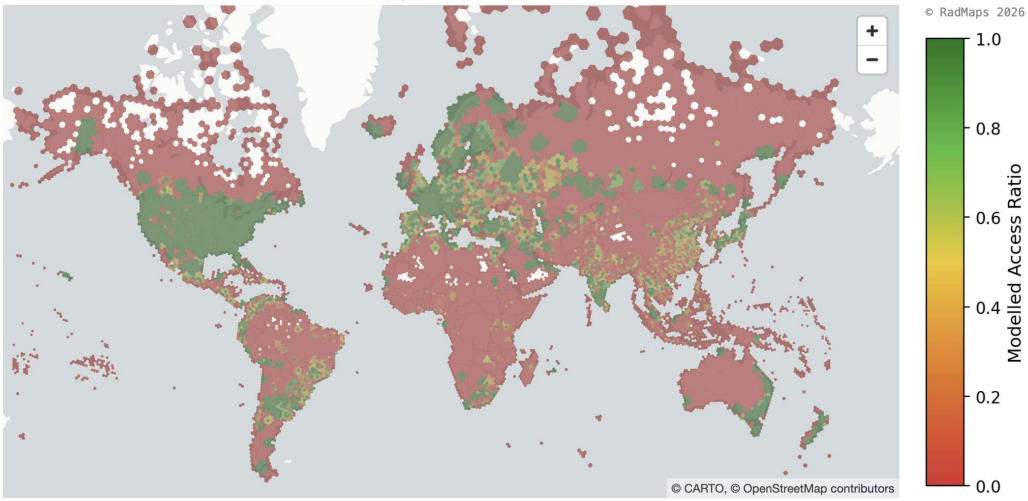
Figure 2: Global distribution of population density and radiotherapy demand at H3 Resolution-3. Each blue cylinder represents a radiotherapy facility, with the height of the cylinder proportional to the number of linacs in the facility.

the lack of machines across Africa, Asia, Indonesia, South America, and rural Australia.

A comparison of the three different radiotherapy access metrics discussed in this paper as applied to this global anaylsis is presented in Table 1. Evaluating capacity alone gives $A_{\mathrm{C}} = 70\,\%$, indicating that a $30\,\%$ gap in global



(a) Deficit per hexagon, Δ_h.



(b) Access ratio per hexagon, A_h/D_h.

Figure 3: Global distribution of radiotherapy deficit and access ratio at H3 Resolution-3. Results obtained by simulating each country individually and assuming a 200 km step-function threshold for access for each facility.

demand remains unaddressed, equating to a deficit of approximately 7,000 machines. The geography-only baseline of $A_{\mathrm{G}} = 91\,\%$ demonstrates that the vast majority of the global population lives within 200 km of at least one facility. Critically, however, the combined RadMaps metric $\mathrm{A_{RM}} = 60\,\%$ is significantly lower than either standalone metric. This difference captures a

critical spatial mismatch: global radiotherapy deficits are not merely driven by an absolute shortage of equipment, but by an unequal distribution of that treatment capacity - a nuance that neither individual metric can isolate.

Table 1: Global radiotherapy access metrics at H3 Resolution-3 with a 200 km step-function threshold.

	$\mathbf{A_C}$	$\mathbf{A_G}$	$\mathbf{A_{RM}}$
Global	70.0%	91.0%	59.9%

3.2. National Analysis

Table 2 shows the population, cancer incidence, and number of radiotherapy facilities and linacs for the six analysed countries. The wide variation in cancer incidence between countries reflects the well-documented correlation between incidence rates and human development index (Fidler et al., 2016, 2019).

Table 2: National baseline statistics: population, cancer incidence, and facility inventory.

Country	**Pop (M)**	**Inc (k)**	**Inc (%)**	$N_{\mathbf{fac}}$	$N_{\mathbf{lin}}$
Australia	26.4	151.5	0.57	103	224
India	1430.2	1401.7	0.10	457	800
Nigeria	224.1	124.7	0.06	12	17
Oman	4.7	4.0	0.09	2	7
United Kingdom	67.7	417.5	0.62	73	358
United States	340.2	1832.6	0.54	2202	3904

Table 3 shows the radiotherapy demand (D) assuming the optimal RTU, alongside the capacity-only (A_C), geography-only (A_G), and RadMaps (A_{RM}) access metrics for each of the six countries. The geography and RadMaps metric assume a step-function with a 2 h driving time cut-off and are calculated at H3 Resolution-5 (cell areas ranging from 154 km^2 to 305 km^2 with an average edge length of 9.9 km).

Plotting these access metrics as a percentage of demand in Figure 4 reveals distinct country profiles. Australia and the United States represent

Table 3: National radiotherapy access metrics by country and travel modality, at H3 Resolution-5 with a 2 h step-function threshold.

Country	D **(k)**	$\mathbf{A_C}$ (k)	$\mathbf{A_G}$ $(k)^\dagger$	$\mathbf{A_{RM}}$ $(k)^\dagger$
Australia	82.3	82.3	77.0	76.3
India	785.8	360.0	461.7	279.3
Nigeria	75.5	7.7	17.5	7.2
Oman	2.3	2.3	1.1	1.1
United Kingdom	238.7	161.1	237.3	161.1
United States	1041.6	1041.6	1028.9	1019.2

† *Geographic and RadMaps metrics based on a* 2 h *driving time.*

high-access profiles where all three metrics are high. The United Kingdom represents a capacity-constrained profile, where the geographic of its radiotherapy infrastructure relative to the demand is very high, but its absolute equipment capacity is insufficient. Conversely, Oman represents a geographically-constrained profile; while its theoretical capacity is sufficient to meet total national demand, geographic access to its facilities remains low. Finally, India and Nigeria represent doubly-constrained profiles, where both absolute capacity and geographical distribution are lacking. Notably, the further drop in A_{RM} for India indicates that its existing capacity is unevenly distributed relative to demand.

Alongside maps visualising the local deficit Δ_h and local access ratio A_h/D_h in Appendix Appendix A, we present an analysis of each country in further detail below.

Australia (Figure A.1). Australia has sufficient capacity to meet its radiotherapy demand in full. Furthermore, despite the country's vast size, only 7 % of its population lives more than 2 h from one of its 103 radiotherapy facilities. The close mirroring between $\mathrm{A_{RM}}$ and $\mathrm{A_G}$ reflects that its capacity is well-distributed relative to the local demand, with the remaining deficit largely scattered across coastal populations rather than concentrated in any single region.

India (Figure A.2). India has a theoretical capacity sufficient to only meet 46% of its total demand. This absolute shortage is further compounded by geographic constraints as only 59 % of the population lives within a 2 h

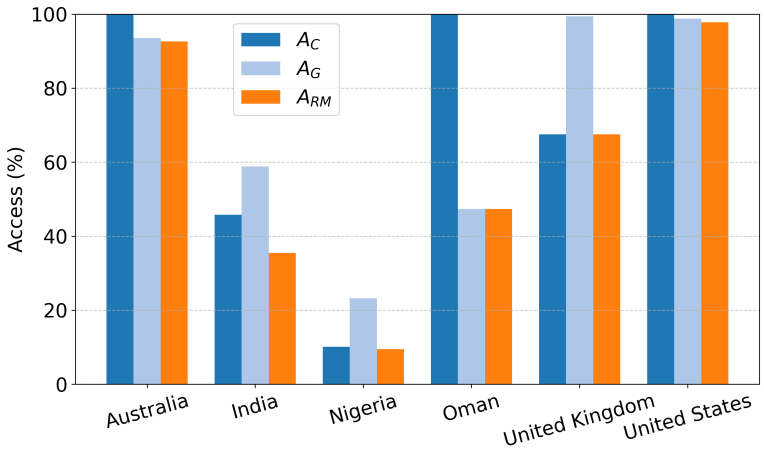


Figure 4: The capacity-only (A_C), geography-only (A_G), and RadMaps (A_{RM}) radiotherapy access metrics as a percentage of demand for the six analysed countries.

drive of a radiotherapy centre. Furthermore, the significant drop in the combined RadMaps metric to 35 % suggests a maldistribution of this capacity. Facilities are particularly lacking in the high-density Uttar Pradesh and Bihar regions in the northeast.

Nigeria (Figure A.3). Nigeria possesses a theoretical capacity to meet only 10 % of its national demand. Additionally, only 23 % of the population lives within a 2 h drive of a centre, driven by the fact that the country has just 12 radiotherapy facilities. The close alignment between A_{RM} and A_C indicates saturation of existing infrastructure, with every machine already operating at its maximum throughput of 450 patients per year. Additional machines and facilities are particularly required in Lagos in the southwest, Kano in the north, and the major urban centres throughout the southeast.

Oman (Figure A.4). While Oman has sufficient theoretical capacity to meet its national demand, its 7 linacs are all located within 2 radiotherapy centres in Muscat in the northeast. Consequently, Oman represents a clear geographically-constrained profile, where only 47 % of the population lives within a 2 h drive of a center. As a result, the remaining access deficit appears most strongly in urban regions in the southwest as well as the northernmost regions of the country.

United Kingdom (Figure A.5). Radiotherapy centres are well distributed across the United Kingdom, with 99 % of the population living within a 2 h drive of a facility. There is, however, insufficient absolute capac-

ity, with only enough machines to meet 68 % of the demand. The mirroring of the combined RadMaps metric A_{RM} to the capacity-only baseline A_C reflects that additional machines are required throughout the entire country, with the deficit particular acute throughout England.

United States (Figure A.6). The United States possesses a substantial overall capacity that exceeds demand by more than 70 %. This capacity is well distributed geographically with 98 % of the population living within a 2 h drive of a facility. The primary region of deficit within the contiguous United States occurs in southern Texas along the border with Mexico, while Puerto Rico stands out as a significant regional contributor, accounting for a deficit of roughly 10,000 patients alone (1 % of the total national demand).

4. Discussion

RadMaps demonstrates the value of simultaneously modelling capacity and geographic constraints on radiotherapy access to produce a combined metric that reveals access deficits not captured by either constraint alone. The global analysis illustrates this clearly whereby capacity-only access of 70 % and geography-only access of 91 % simulated together yield a combined access of only 60 %, underscoring how the two constraints compound in ways that neither metric alone can capture. The national analyses further demonstrate the tool's ability to distinguish qualitatively distinct access profiles and localise deficits at sub-national scale, pointing towards whether investment should prioritise additional capacity, new facility locations, or both.

RadMaps nonetheless relies on a number of assumptions that must be considered when interpreting results.

Uniform cancer incidence. RadMaps distributes cancer incidence uniformly across the population, such that the radiotherapy demand within each hexagon is directly proportional to its share of the national population. In practice, cancer risk varies spatially within countries due to demographic differences (for example, older, more urbanised, or more deprived populations tend to have higher incidence rates (Brown et al., 2018; Wild et al., 2020)) meaning that demand may be systematically under- or over-estimated in certain regions. This limitation could be addressed by incorporating sub-national cancer incidence data where available.

No patient stratification. All radiotherapy demand is treated as equivalent, whereas in practice the specific radiotherapy modality and type of

treatment required can vary by cancer type, disease stage, patient age, mobility, and due to socioeconomic reasons. These treatment factors, in turn, alter the actual demand for access and stratifying demand by these factors would improve the model.

Geographic access model. There is no empirical model on the relationship between travel distance or time and radiotherapy uptake or treatment outcome. While RadMaps offers three configurable decay models, the choice of model and parameters can significantly affect results. Further research into context-specific access-decay functions would strengthen the evidence base for model parameterisation.

Greedy nearest-first allocation. RadMaps assumes that each facility serves its nearest patients first, whereas real referral patterns may depend on clinical pathways, waiting times, institutional capacity, and patient choice. This assumption makes RadMaps computationally efficient and provides a reasonable first-order approximation, but may overestimate access in settings where referral patterns diverge significantly from geographic proximity.

Interpretation. RadMaps has not yet been benchmarked against observed radiotherapy uptake, and the access metrics should therefore be interpreted as modelled proxies rather than empirical measures of realised access. Future validation against national or regional utilisation data is essential in establishing the tool's predictive validity.

Additional assumptions worth noting include: the use of incident (new) cancer cases only, which exclude patients requiring retreatment; treating all DIRAC MVMs as equivalent linacs; applying national boundaries as hard limits on patient flow; treating private and public facilities equally; and the inherent limitations of the underlying datasets, particularly the DIRAC database which may not fully capture recent facility openings or closures.

Notwithstanding these limitations, RadMaps provides a flexible and computationally efficient framework for radiotherapy access modelling that can be applied consistently across any country or region. The modular design allows the underlying datasets and model parameters to be updated as better data become available, and the tool is freely accessible via a Streamlit web application and open-source GitHub repository. Beyond radiotherapy, the framework is readily adaptable to access modelling for other healthcare facilities and services where capacity and geographic constraints interact.

5. Conclusion

RadMaps is an open-source geospatial framework that simultaneously models capacity and geographic constraints on radiotherapy access, producing a combined access metric that captures the compounding effect of both constraints at sub-national scale. Applied globally and across six countries, the tool demonstrates its ability to distinguish qualitatively distinct access profiles and localise deficit hotspots, pointing towards where radiotherapy infrastructure investment may be most needed. The modular framework is freely available and readily extensible, providing a foundation for larger-scale analyses of radiotherapy access and broader access modelling across diverse geographic and socioeconomic contexts.

While this paper describes the methodology underpinning RadMaps, the tool is actively being distributed to healthcare professionals and radiotherapy planners to evaluate its practical utility and to validate modelled access metrics against observed treatment uptake data. This engagement will inform future development of the tool and establish the evidence base for its use in infrastructure planning and policy prioritisation.

List of Abbreviations

API: Application Programming Interface **DIRAC:** Directory of Radiotherapy Centres **EBRT:** External Beam Radiotherapy **GLOBOCAN:** Global Cancer Observatory **H3:** Hexagonal Hierarchical Geospatial Indexing System **IAEA:** International Atomic Energy Agency **MVM:** Megavoltage Machine **RT:** Radiotherapy **RTU:** Radiotherapy Utilisation

Declarations

Acknowledgements

The authors are thankful to TravelTime who provided extended API-usage and assistance with incorporating their data into the model, and Walter Wuensch for feedback on the manuscript.

Data Availability

This study uses publicly aggregated and accessible data. The data is available on the RadMaps GitHub `https://github.com/LaurenceWroe/Geospatial-modelling-radiotherapy-access`.

Ethics approval and consent to participate

Not applicable.

Consent for publication

Not applicable.

Competing interests

The authors declare no competing interests.

Funding

Not applicable.

Authors' contributions

LW: Conceptualisation; Data curation; Investigation; Methodology; Supervision; Validation; Visualisation; Writing - original draft; Writing - review & editing.

AB: Data curation; Investigation; Visualisation; Writing - review & editing.

AH: Data curation; Investigation; Visualisation; Writing - review & editing.

SM: Data curation; Investigation; Visualisation; Writing - review & editing.

SS: Supervision; Writing - review & editing.

References

Peter D Baade, Paramita Dasgupta, Joanne F Aitken, and Gavin Turrell. Distance to the closest radiotherapy facility and survival after a diagnosis of rectal cancer in queensland. *Medical Journal of Australia*, 195(6):350–354, 2011. doi: https://doi.org/10.5694/mja10.11204. URL `https://onlinelibrary.wiley.com/doi/abs/10.5694/mja10.11204`.

Michael B. Barton, Susannah Jacob, Jesmin Shafiq, Karen Wong, Stephen R. Thompson, Timothy P. Hanna, and Geoff P. Delaney. Estimating the demand for radiotherapy from the evidence: A review of changes from 2003 to 2012. *Radiotherapy and Oncology*, 112(1):140–144, 2014. ISSN 0167-8140. doi: https://doi.org/10.1016/j.radonc.2014.03.024. URL `https://www.sciencedirect.com/science/article/pii/S0167814014001698`.

Freddie Bray, Mathieu Laversanne, Hyuna Sung, Jacques Ferlay, Rebecca L. Siegel, Isabelle Soerjomataram, and Ahmedin Jemal. Global cancer statistics 2022: Globocan estimates of incidence and mortality worldwide for 36 cancers in 185 countries. *CA: A Cancer Journal for Clinicians*, 74(3):229–263, 2024. doi: https://doi.org/10.3322/caac.21834. URL `https://acsjournals.onlinelibrary.wiley.com/doi/abs/10.3322/caac.21834`.

Katrina F. Brown, Harriet Rumgay, Catherine Dunlop, Michael Ryan, Robert Quartly, Amanda Cox, Anne Deas, Ruth Lyon, Lynn Beattie, Rowena Oliphant, Rebecca Ormiston-Rees, Gini Samuel, Claire White, and Donald Max Parkin. The fraction of cancer attributable to modifiable risk factors in England, Wales, Scotland, Northern Ireland, and the United Kingdom in 2015. *British Journal of Cancer*, 118(8):1130–1141, 2018. doi: 10.1038/s41416-018-0029-6. URL `https://doi.org/10.1038/s41416-018-0029-6`.

CartoDB. Carto basemap styles license. `https://github.com/CartoDB/basemap-styles/blob/master/LICENSE.md`, 2018.

Geoff Delaney, Susannah Jacob, Carolyn Featherstone, and Michael Barton. The role of radiotherapy in cancer treatment. *Cancer*, 104(6):1129–1137, 2005. doi: https://doi.org/10.1002/cncr.21324. URL `https://acsjournals.onlinelibrary.wiley.com/doi/abs/10.1002/cncr.21324`.

Peter Dunscombe, Cai Grau, Noémie Defourny, Julian Malicki, Josep M. Borras, Mary Coffey, Marta Bogusz, Chiara Gasparotto, Ben Slotman, Yolande Lievens, Arianit Kokobobo, Felix Sedlmayer, Elena Slobina, Olivier De Hertogh, Tatiana Hadjieva, Jiri Petera, Jesper Grau Eriksen, Jana Jaal, Ritva Bly, David Azria, Michael Baumann, Zoltan Takacsi-Nagy, Jakob Johannsson, Moya Cunningham, Stefano Magrini, Vydmantas Atkocius, Michel Untereiner, Martin Pirotta, Vanja Karadjinovic, Sverre Levernes, Marian Reinfuss, Maria Lurdes Trigo, Valentin Cernea, Pavol Dubinsky, Šegedin Barbara, Jose Lopez Torrecilla, Bert Pastoors, Roger Taylor, and Scott Taylor. Guidelines for equipment and staffing of radiotherapy facilities in the european countries: Final results of the estro-hero survey. *Radiotherapy and Oncology*, 112(2):165–177, 2014. ISSN 0167-

8140. doi: https://doi.org/10.1016/j.radonc.2014.08.032. URL https://www.sciencedirect.com/science/article/pii/S0167814014003624.

Miranda M. Fidler, Isabelle Soerjomataram, and Freddie Bray. A global view on cancer incidence and national levels of the human development index. *International Journal of Cancer*, 139(11):2436–2446, 2016. doi: https://doi.org/10.1002/ijc.30382. URL https://onlinelibrary.wiley.com/doi/abs/10.1002/ijc.30382.

Miranda M. Fidler, Salvatore Vaccarella, and Freddie Bray. Social inequalities in cancer between countries. In Salvatore Vaccarella, Joannie Lortet-Tieulent, Rodolfo Saracci, et al., editors, *Reducing social inequalities in cancer: evidence and priorities for research*, number 168 in IARC Scientific Publications, chapter 5. International Agency for Research on Cancer, Lyon (FR), 2019. URL https://www.ncbi.nlm.nih.gov/books/NBK566196/.

Sharad Goyal, Sheenu Chandwani, Bruce G. Haffty, and Kitaw Demissie. Effect of travel distance and time to radiotherapy on likelihood of receiving mastectomy. *Annals of Surgical Oncology 2014 22:4*, 22:1095–1101, 9 2014. ISSN 15344681. doi: 10.1245/s10434-014-4093-8. URL https://link.springer.com/article/10.1245/s10434-014-4093-8.

B.J. Healy, D. van der Merwe, K.E. Christaki, and A. Meghzifene. Cobalt-60 machines and medical linear accelerators: Competing technologies for external beam radiotherapy. *Clinical Oncology*, 29(2):110–115, 2017. ISSN 0936-6555. doi: https://doi.org/10.1016/j.clon.2016.11.002. URL https://www.sciencedirect.com/science/article/pii/S0936655516303995. SI: Radiotherapy in low and middle income countries.

International Atomic Energy Agency. The iaea directory of radiotherapy centres (dirac). https://dirac.iaea.org/, 2025. Accessed July 2025.

Kontur, Inc. Kontur population dataset. https://www.kontur.io/portfolio/population-dataset/, November 2023. H3 hexagonal grid resolution 8 (0.74 km^2). Accessed 2025.

Fabio Y. Moraes, Andre G. Gouveia, Vanessa Freitas Bratti, Edward C. Dee, Juliana Fernandes Pavoni, Laura M. Carson, Cecília Félix Penido Mendes

de Sousa, Richard Sullivan, Gustavo Nader Marta, Wilma M. Hopman, Christopher M. Booth, Ajay Aggarwal, Ahmedin Jemal, Timothy P. Hanna, Brooke E. Wilson, and Gustavo Arruda Viani. Global linear accelerator requirements and personalised country recommendations: a cross-sectional, population-based study. *The Lancet Oncology*, 26:239–248, 2 2025. ISSN 14745488. doi: 10.1016/S1470-2045(24)00678-8.

Sierra M. Silverwood, Kathleen Waeldner, Sasha K. Demeulenaere, Shavit Keren, Jason To, Jie Jane Chen, Zakaria El Kouzi, Alan Ayoub, Surbhi Grover, Katie E. Lichter, and Osama Mohamad. The relationship between travel distance for treatment and outcomes in patients undergoing radiation therapy: A systematic review. *Advances in Radiation Oncology*, 9:101652, 12 2024. ISSN 24521094. doi: 10.1016/j.adro.2024.101652. URL https://www.advancesradonc.org/action/showFullText?pii=S245210942400215Xhttps://www.advancesradonc.org/action/showAbstract?pii=S245210942400215Xhttps://www.advancesradonc.org/article/S2452-1094(24)00215-X/abstract.

TravelTime. TravelTime API documentation, 2026. URL https://docs.traveltime.com/api/overview/introduction. Accessed: 2026-04-01.

Melanie Turner, Romi Carriere, Shona Fielding, George Ramsay, Leslie Samuel, Andrew Maclaren, and Peter Murchie. The impact of travel time to cancer treatment centre on post-diagnosis care and mortality among cancer patients in scotland. *Health & Place*, 84:103139, 2023. ISSN 1353-8292. doi: https://doi.org/10.1016/j.healthplace.2023.103139. URL https://www.sciencedirect.com/science/article/pii/S1353829223001764.

Melanie Turner, Samuel Kent, Sharon Hanley, and Peter Murchie. Exploring associations between travel burden, clinical features, and outcomes from head and neck cancer in scotland, uk. *Cancer Epidemiology*, 101:103012, 2026. ISSN 1877-7821. doi: https://doi.org/10.1016/j.canep.2026.103012. URL https://www.sciencedirect.com/science/article/pii/S1877782126000275.

Uber. h3: Hexagonal hierarchical geospatial indexing system. https://github.com/uber/h3, 2025.

Dominik Wawrzuta, Justyna Klejdysz, Katarzyna Pędziwiatr, and Marzanna Chojnacka. Global access to radiotherapy: A geospatial analysis of current disparities and optimal facility placement. *Radiotherapy and Oncology*, 211, 10 2025. ISSN 18790887. doi: 10.1016/j.radonc.2025.111061. URL https://www.thegreenjournal.com/action/showFullText?pii=S0167814025045657https://www.thegreenjournal.com/action/showAbstract?pii=S0167814025045657https://www.thegreenjournal.com/article/S0167-8140(25)04565-7/abstract.

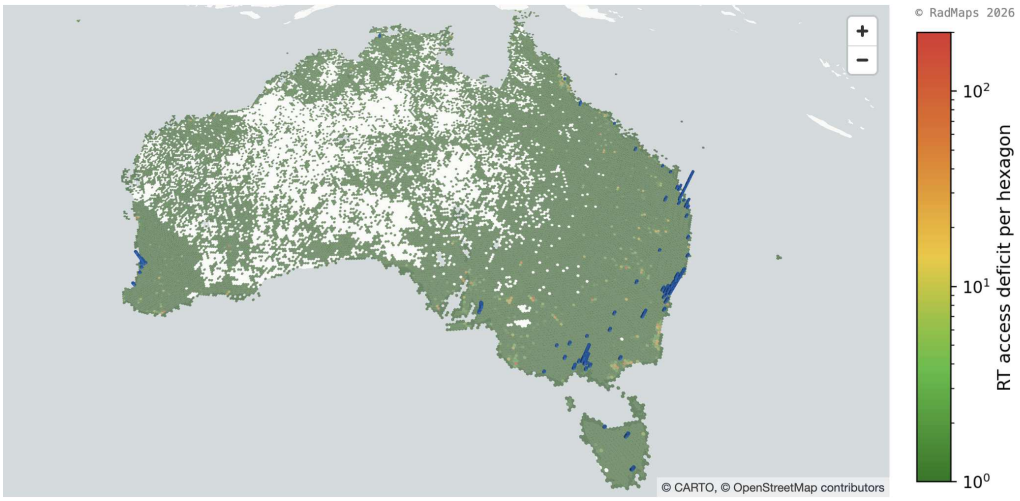
Christopher P. Wild, Elisabete Weiderpass, and Bernard W. Stewart, editors. *World Cancer Report: Cancer Research for Cancer Prevention*. International Agency for Research on Cancer, Lyon (FR), 2020. ISBN 978-92-832-0448-0. URL https://www.ncbi.nlm.nih.gov/books/NBK606505/.

E. H. Zubizarreta, E. Fidarova, B. Healy, and E. Rosenblatt. Need for radiotherapy in low and middle income countries – the silent crisis continues. *Clinical Oncology*, 27:107–114, 2 2015. ISSN 14332981. doi: 10.1016/j.clon.2014.10.006.

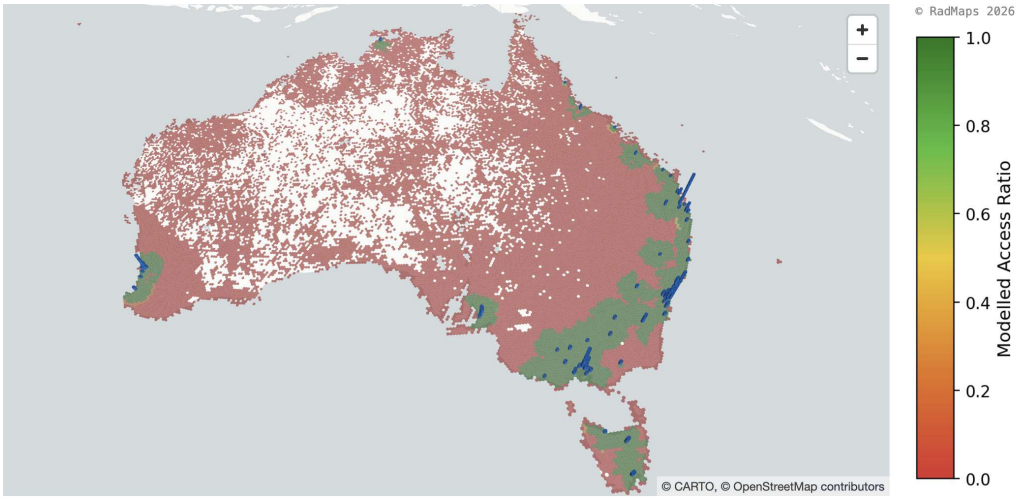
Appendix A. Access Maps

In all radiotherapy deficit plots, the colourbar scale is normalised between 1 and 200 patients per hexagon to allow direct comparison between countries.

Appendix A.1. Australia



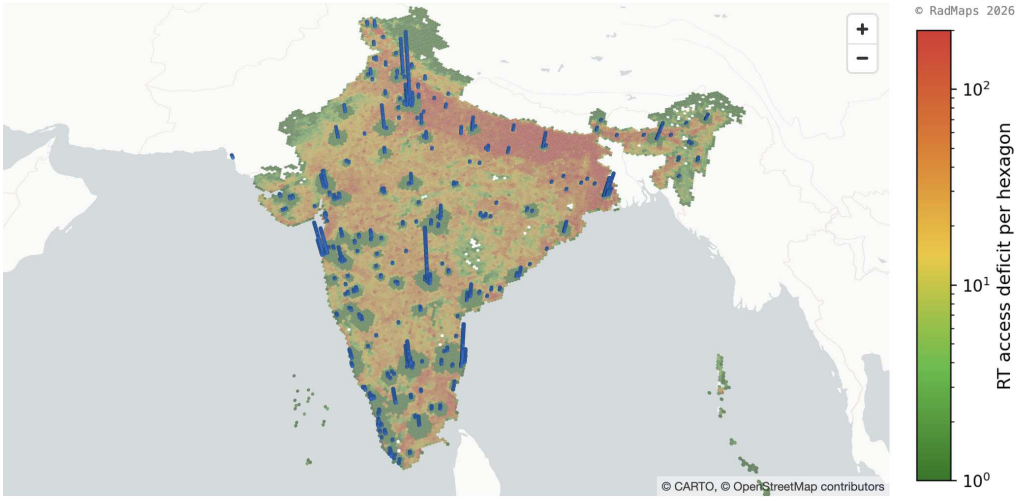
(a) Deficit per hexagon, Δ_h.



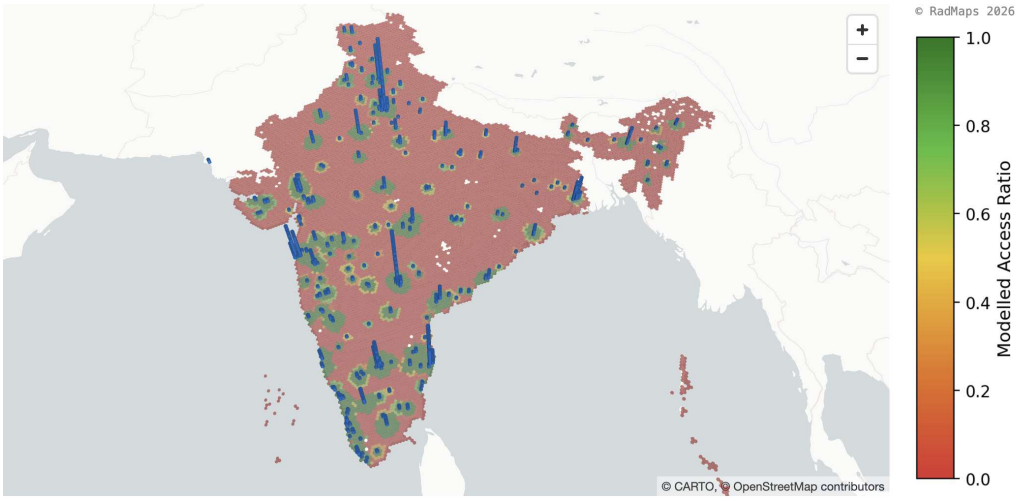
(b) Access ratio per hexagon, A_h/D_h.

Figure A.1: Distribution of radiotherapy deficit and access ratio across Australia at H3 Resolution-5. Calculation assumes a 2 h driving time travel threshold, 450 patients per linac, and an optimal RTU. Each blue cylinder represents a radiotherapy facility, with the height proportional to the number of linacs.

Appendix A.2. India



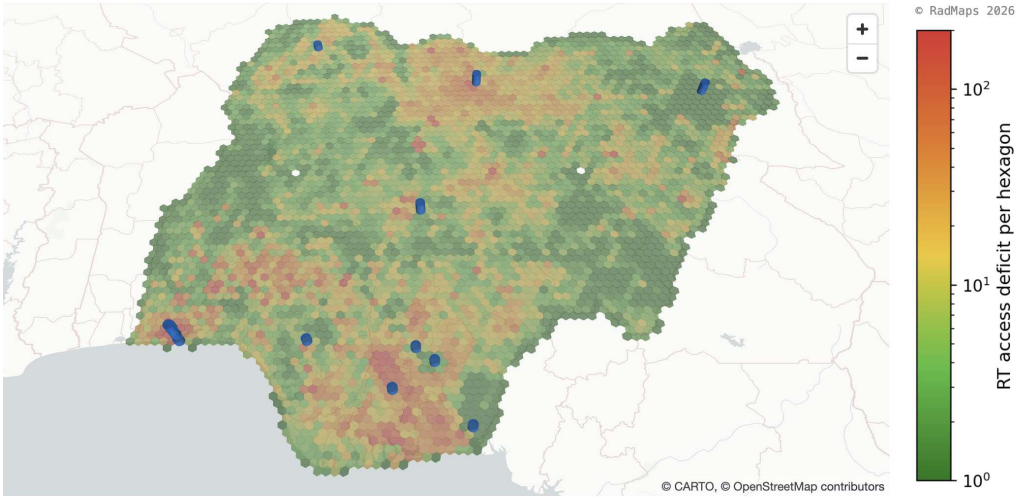
(a) Deficit per hexagon, Δ_h.



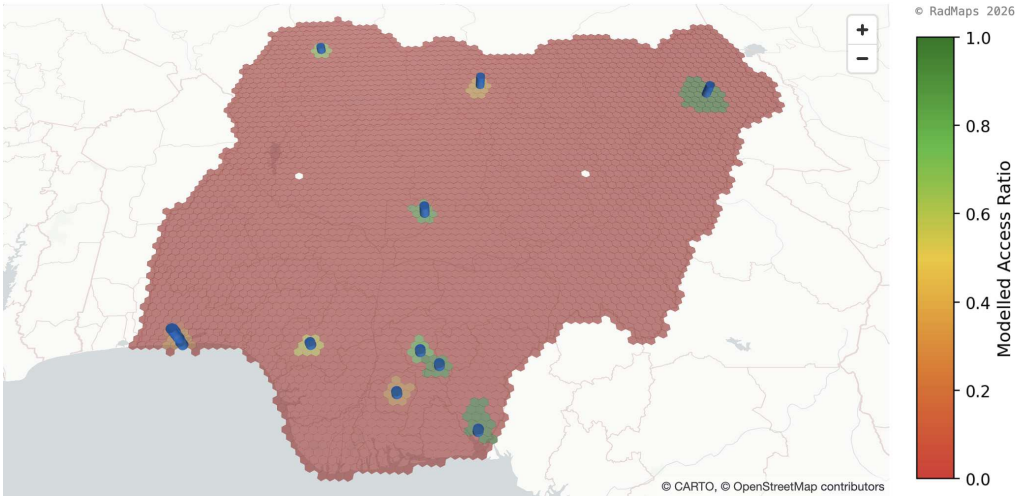
(b) Access ratio per hexagon, A_h/D_h.

Figure A.2: Distribution of radiotherapy deficit and access ratio across India at H3 Resolution-5. Calculation assumes a 2 h driving time travel threshold, 450 patients per linac, and an optimal RTU. Each blue cylinder represents a radiotherapy facility, with the height proportional to the number of linacs.

Appendix A.3. Nigeria



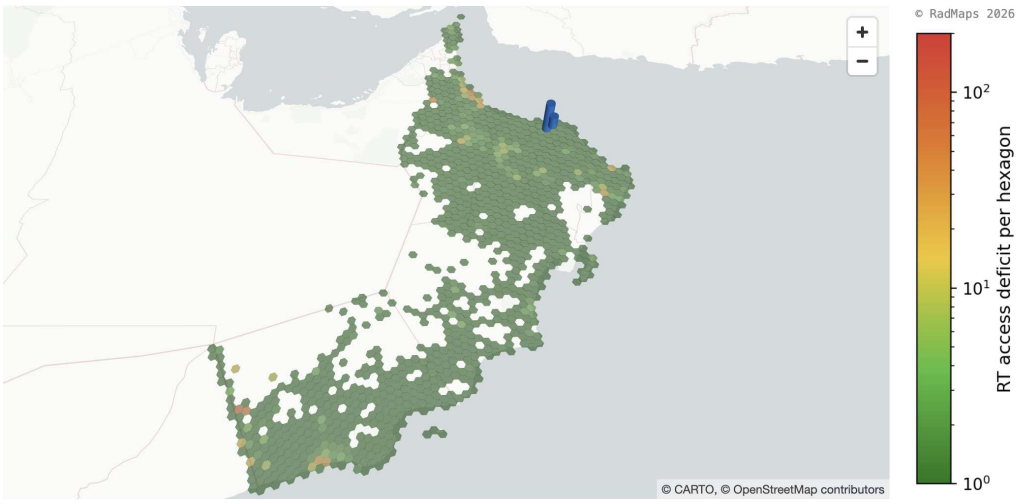
(a) Deficit per hexagon, Δ_h.



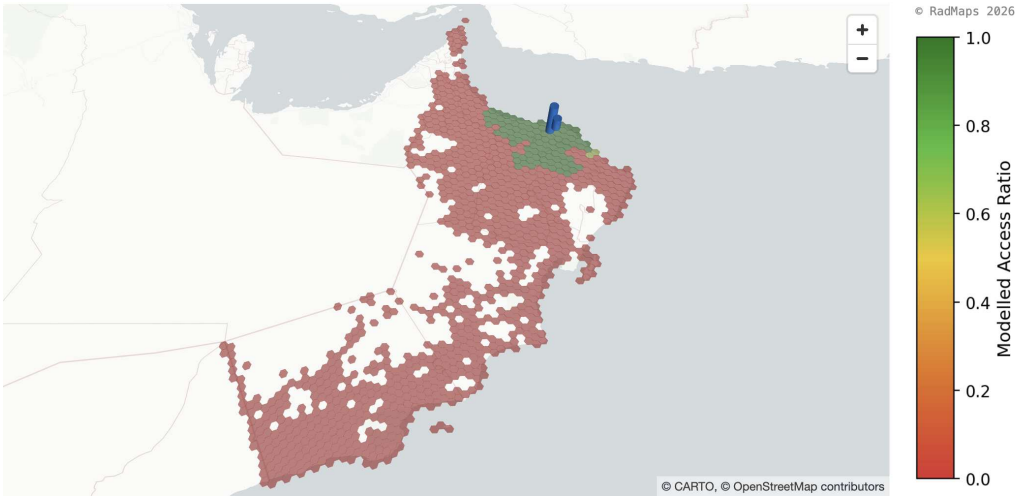
(b) Access ratio per hexagon, A_h/D_h.

Figure A.3: Distribution of radiotherapy deficit and access ratio across Nigeria at H3 Resolution-5. Calculation assumes a 2 h driving time travel threshold, 450 patients per linac, and an optimal RTU. Each blue cylinder represents a radiotherapy facility, with the height proportional to the number of linacs.

Appendix A.4. Oman



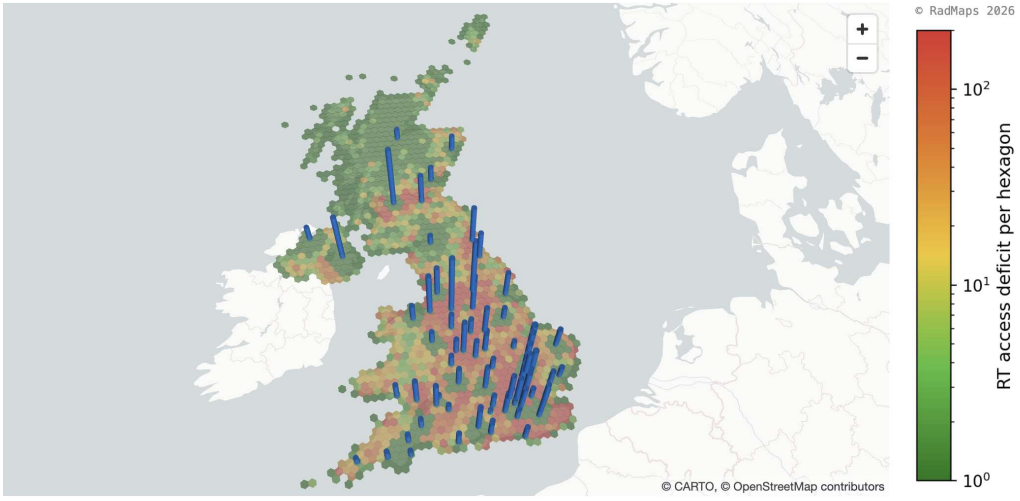
(a) Deficit per hexagon, Δ_h.



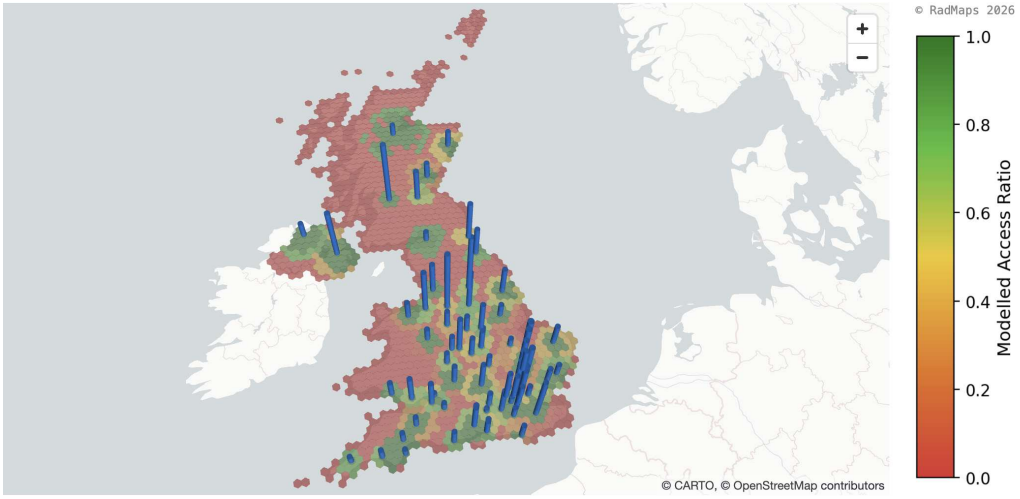
(b) Access ratio per hexagon, A_h/D_h.

Figure A.4: Distribution of radiotherapy deficit and access ratio across Oman at H3 Resolution-5. Calculation assumes a 2 h driving time travel threshold, 450 patients per linac, and an optimal RTU. Each blue cylinder represents a radiotherapy facility, with the height proportional to the number of linacs.

Appendix A.5. United Kingdom



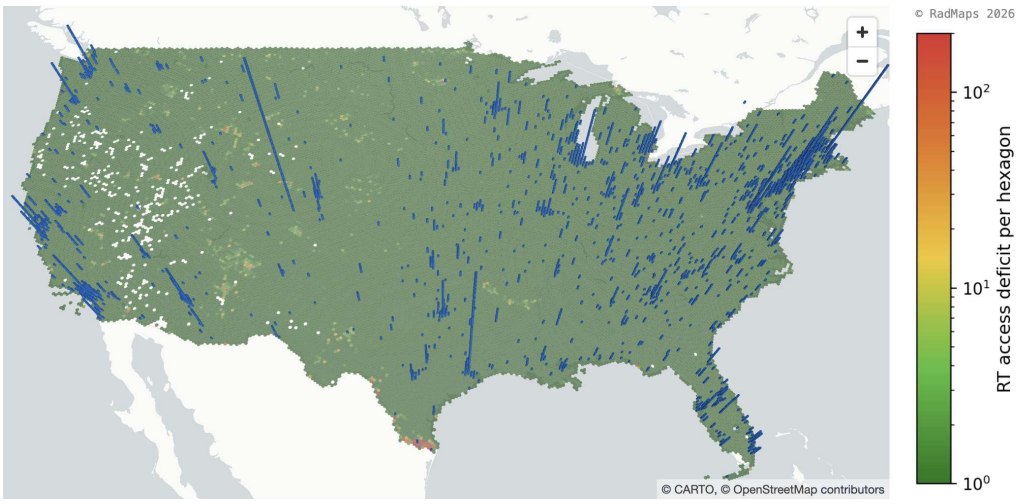
(a) Deficit per hexagon, Δ_h.



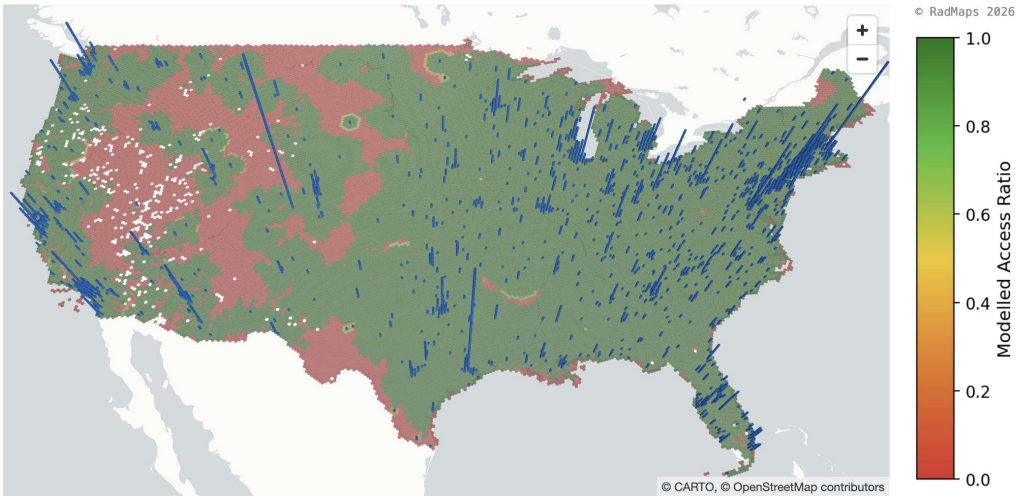
(b) Access ratio per hexagon, A_h/D_h.

Figure A.5: Distribution of radiotherapy deficit and access ratio across the United Kingdom at H3 Resolution-5. Calculation assumes a 2 h driving time travel threshold, 450 patients per linac, and an optimal RTU. Each blue cylinder represents a radiotherapy facility, with the height proportional to the number of linacs.

Appendix A.6. United States



(a) Deficit per hexagon, Δ_h.



(b) Access ratio per hexagon, A_h/D_h.

Figure A.6: Distribution of radiotherapy deficit and access ratio across the contiguous United States at H3 Resolution-5. Calculation assumes a 2 h driving time travel threshold, 450 patients per linac, and an optimal RTU. Each blue cylinder represents a radiotherapy facility, with the height proportional to the number of linacs.